Family Systems of Advanced Charring Ablators for Planetary Aerocapture and Entry Missions

William M. Congdon
ARA Ablatives Laboratory
Applied Research Associates, Inc.
14824 E. Hinsdale Avenue
Centennial, Colorado 80112

Abstract - Family systems of ablators are being matured and readied for flight infusion under the sponsorship of the NASA ISPT project. These are silicone and phenolic families each with a broad range of density and performance for the diverse heating environments of future planetary science missions. Subscale 1.0-m ablative aeroshells are being produced to mature TPS manufacturing and system-level tests of these ablative aeroshells are validating their thermostructural integrity.

I. INTRODUCTION

During the past four years, the ARA Ablatives Laboratory has been conducting performance characterization testing and production scale-up testing of new family systems of advanced charring ablators [1-3]. The primary application is future aerocapture and direct-entry missions to the planets and to the moon Titan, where severe atmospheric heating requires charring-ablator TPS [4-5]. This effort starting in 2003 has been sponsored by NASA's In-Space Propulsion Technology Project [6], now managed by the NASA Glenn Research Center. With a long development history that started more than ten years back, these advanced family systems consist of silicone ablators with densities ranging from 14.0 lb/ft^3 to 24.0 lb/ft^3 (0.22 g/cm^3 to 0.38 g/cm^3) and phenolic-carbon ablators with densities from 20.0 lb/ft^3 to 36.0 lb/ft^3 (0.32 g/cm^3 to 0.58 g/cm^3). The higher density phenolic ablators are suitable for heating environments up to more than 1000 W/cm^2, whereas the silicone materials, which are better insulators with simpler manufacturing, are recommended for heating rates up to about 300 to 400 W/cm^2. The ablators are reinforced with internal fibers and also with large-cell honeycomb of 1.0-in. (2.54-cm) cell size into which the mixed ablator compound is pressure packed and then cured. Alternate manufacturing methods besides the honeycomb packing approach (HCPA) are the strip-collar bonding approach (SCBA) and monolithic production and application. This paper summarizes some results of the extensive ablator arc-jet testing and thermal radiation testing performed under the ISPT project over four years of effort. It also discusses the manufacturing of 1.0-meter demonstration aeroshells and system-level thermostructural testing of ablators over lightweight sandwich composite structures. Much of this discussion centers on the Ablatives Laboratory's SRAM-20 ablator, a 20 lb/ft^3 (0.32 g/cm^3) silicone material that was competitively selected and baselined by NASA in 2006 for a possible Earth-return demonstration flight of aerocapture technology [7]. A photo of SRAM-20 undergoing ablation testing in the NASA/ARC IHF arc-jet is shown in Figure 1.

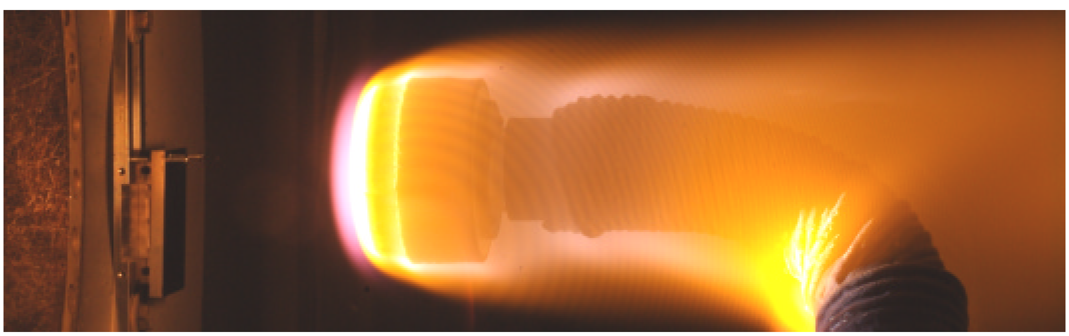

Fig. 1 - SRAM-20 Ablator Sample In Test at 153 W/cm^2 in IHF Arc-Jet at NASA/ARC

II. TECHNICAL DISCUSSION

A. Family Systems of Ablators

Two of the Ablatives Laboratory's family systems of advanced charring ablators are summarized in Table 1. These are the silicone-based SRAM system and the phenolic-based PhenCarb system. Having family systems available with similar materials covering a wide range of performance and density facilitates best-ablator selections for specific entry heating environments. Within a family, all members are compacted and cured at the same pressure and temperature, but each member has a unique formulation of the same or similar ingredients. Ablators in both family systems contain density-reducing fillers such as microspheres in addition to reinforcing fibers. This paper focuses on two key ablators that are members selected from each family system. They are SRAM-20 and PhenCarb-28. For the discussions that follow, arc-jet results and performance for these two ablators are representative of their larger family systems.

Table 1 – Ablatives Laboratory Family Systems of Charring Ablators

Ablator	Density	Resin System	Fillers	Heating Range	EDL Location	Abbrv.
SRAM-14	14 lb/ft^3	Silicone	Silica / others	90 to 140 W/cm^2	Forebody	S-14
SRAM-17	17 lb/ft^3	Silicone	Silica / others	120 to 220 W/cm^2	Forebody	S-17
SRAM-20	20 lb/ft^3	Silicone	Silica / others	150 to 300 W/cm^2	Forebody	S-20
SRAM-24	24 lb/ft^3	Silicone	Silica / others	180 to 380 W/cm^2	Forebody	S-24
PhenCarb-20	20 lb/ft^3	Phenolic	Carbon / others	200 to 500 W/cm^2	Forebody	P-20
PhenCarb-24	24 lb/ft^3	Phenolic	Carbon / others	300 to 700 W/cm^2	Forebody	P-24
PhenCarb-28	28 lb/ft^3	Phenolic	Carbon / others	400 to 900 W/cm^2	Forebody	P-28
PhenCarb-32	32 lb/ft^3	Phenolic	Carbon / others	500 to 1100 W/cm^2	Forebody	P-32
PhenCarb-36	36 lb/ft^3	Phenolic	Carbon / others	600 to 1300 W/cm^2	Forebody	P-36

B. SRAM-20 Testing for Earth Aerocapture

Special SRAM-20 arc-jet tests were conducted in 2006 for Earth-aerocapture design studies. Samples had near flight-like ablator and composite structure and contained in-depth thermocouples for response model verification. They were 5.0-in. diameter "iso-q" type samples with a convex surface of 5.0-in. radius. They had 1.30-in. thick ablator over 1.040-in. thick sandwich composite supplied by ATK Space Systems. The Ablator was packed into large-cell silica honeycomb of 1.0-in. cell size. (Large-cell H/C is produced in the Ablatives Laboratory using silica or carbon fabrics.) Each sample had a 1.25-in. diameter ablator plug with in-depth thermocouples set at depths of 0.20, 0.40, 0.60, and 1.20 in. below the local top surface (see Fig.2). Six samples of this type were tested in the IHF arc-jet at NASA/ARC at aerocapture heating rates of 128, 254, and 304 W/cm^2 (two samples at each condition). Results are shown in Figure 3 in the form of posttest sample appearance and measured surface recession for one sample at each heating rate. Recessions for these samples were determined to be zero for the lowest heating rate (Sample 3426) and 0.33 in. and 0.43 in. for the higher rates of Samples 3424 and 3421). In the same sample order, peak bondline temperatures were recorded to be 173ºC, 114ºC and 122ºC. SRAM-20 samples had good performance with excellent thermal insulation and low surface recession.

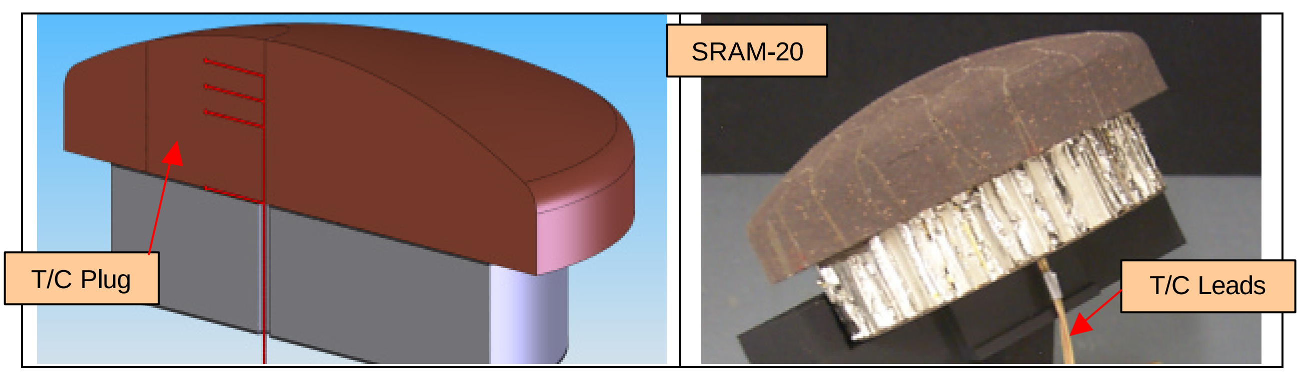

Fig. 2 – SRAM-20 (HCPA) Sample Configuration (5.0-In.) for Earth-Aerocapture Arc-Jet Tests in 2006.

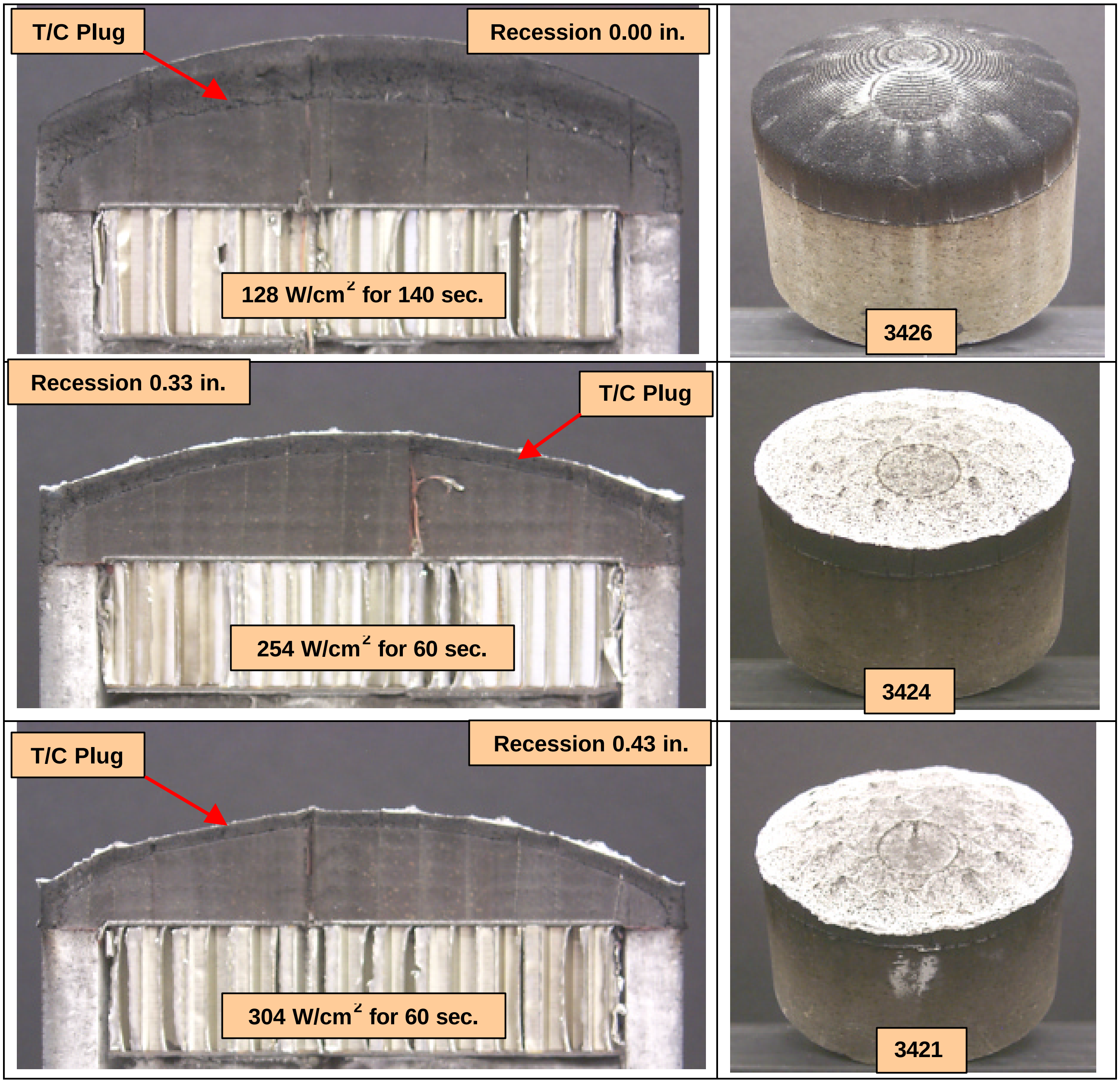

Fig. 3 – Flight-Like 1.30-In. Thick SRAM-20 (HCPA) Ablator Samples Tested in July 2006 for Planned Aerocapture Mission (1.040-In. Thick Composite Structure)

C. SRAM-20 Detailed Discussion

Heated SRAM-20 pyrolyzes to form a durable, reliable char layer, which was a reason for this ablator's selection both in 2006 for Earth aerocapture [7] and also in 2001 as a candidate protective material for the "aerodynamic keel" of the former X-38 vehicle. SRAM-20 was also studied for Mars direct-entry for missions with higher heating than the prior MPF and MER vehicles. The ablator has minimal to no recession for heating rates up to about 130 W/cm^2, but will recede from surface ablation at heating beyond this level. The char layer formed by SRAM-20 is one that can be described as robust. It has good strength and integrity and is almost a *hardshell*. Char density is consistently about 9.4 to 10.4 lb/ft^3 (0.15 to 0.17 g/cm^3). Because of the type of filler materials in its formulation, including carbon-based species, the char has good opacity to thermal radiation. This made S-20 a key heatshield candidate [8] during NASA's 2002-03 studies of future Titan aerocapture missions with entry heating dominated by shock-layer radiation [9-12]

SRAM-20 has been tested and evaluated in the arc-jets of both NASA/JSC and NASA/ARC. Figure 4 shows posttest surface and section photos of SRAM-20 Samples 1544 and 1545 tested in JSC's ARMSEF at 114 W/cm^2 for 100 and 150 sec, respectively. These 4.0-in. diameter samples had an "iso-q" surface of 4.0-in. radius of curvature. They pyrolyzed but did not experience surface "ablation" and posttest measurements indicated no surface recession. They developed thick, durable char layers that can be seen in the photos. (Note that horizontal char split lines seen in the photos are caused by CTE/DTE effects during sample cool-down.)

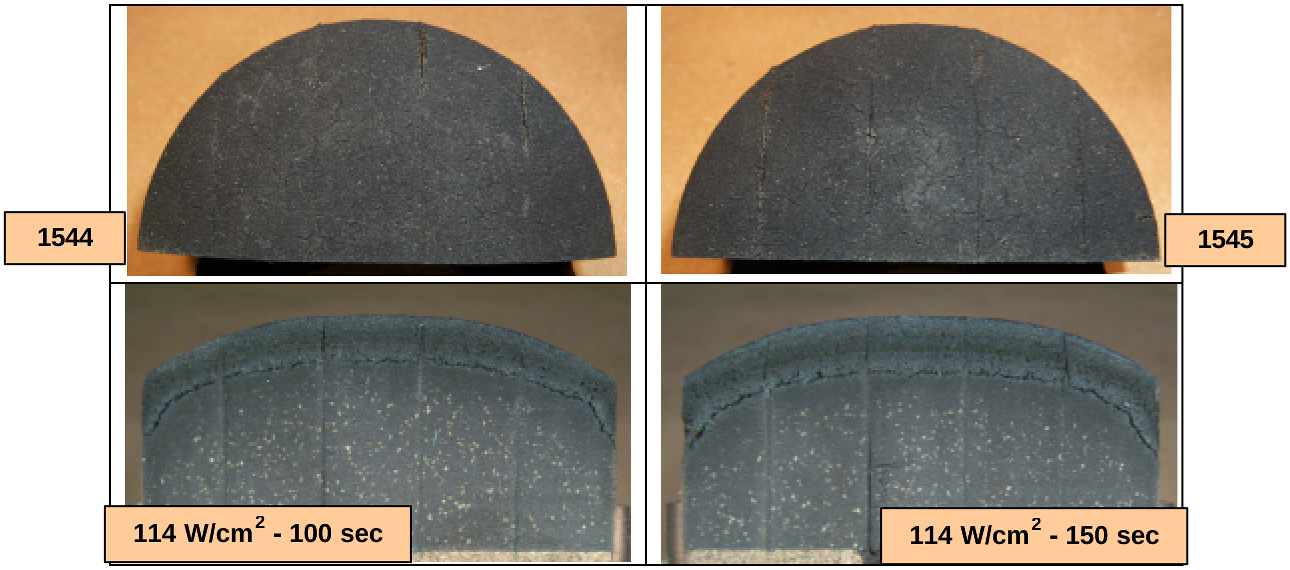

Fig. 4 – SRAM-20 (SCBA) Iso-Q Samples from NASA/JSC ARMSEF Testing at 114 W/cm^2

Figure 5 shows posttest photos of flat-faced SRAM-20 samples (4.0 in.) tested in ARC's IHF arc-jet in 2003. The objective of these samples was to obtain S-20 results at mild ablation conditions where low levels of surface recession would occur. Test conditions were 119 W/cm^2, close to the threshold for surface ablation, and 153 W/cm^2 for moderate ablation. Recession and mass-loss results from testing were correlated to the ablator's thermal response model. Testing was also done at 67 W/cm^2 for validation of the model's thermal conduction properties (properties developed, in part, from earlier testing in ARMSEF). Test results at the near-threshold ablation condition can be seen in the photos of Sample 3002. This sample had essentially zero recession (0.010 in.). At 153 W/cm^2, Sample 3003 had recession of 0.19 in. and Sample 3004 was measured at 0.35 in.

The thermally-formed char layers for Samples 1544, 1545, 3001, and 3002 are thick and strong at ~10 lb/ft^3. Like most ablators, entry-heating accommodation for SRAM-20 is dominated by surface reradiation to space. A thick char layer provides excellent insulation against the high surface temperatures that develop during peak heating. At ablation conditions causing recession, convective energy is also accommodated by surface chemical processes (endothermic) and surface mass injection into the aerodynamic boundary layer. (In-depth pyrolysis and percolating pyrolysis gases also contribute significantly to entry heating accommodation for both non-ablating and ablating conditions.) An interesting feature for flat-faced SRAM-20 samples tested at 153 W/cm^2 is the formed shoulder ridge as seen in the photos of Samples 3003 and 3004. (Also observed in other samples up to heating of 245 W/cm^2.) This is apparently caused by radiation cooling at the shoulder from both conjoining surfaces. Test environments at the shoulder are typically more severe than center locations causing some ablators to spall, but this is not the case for SRAM-20.

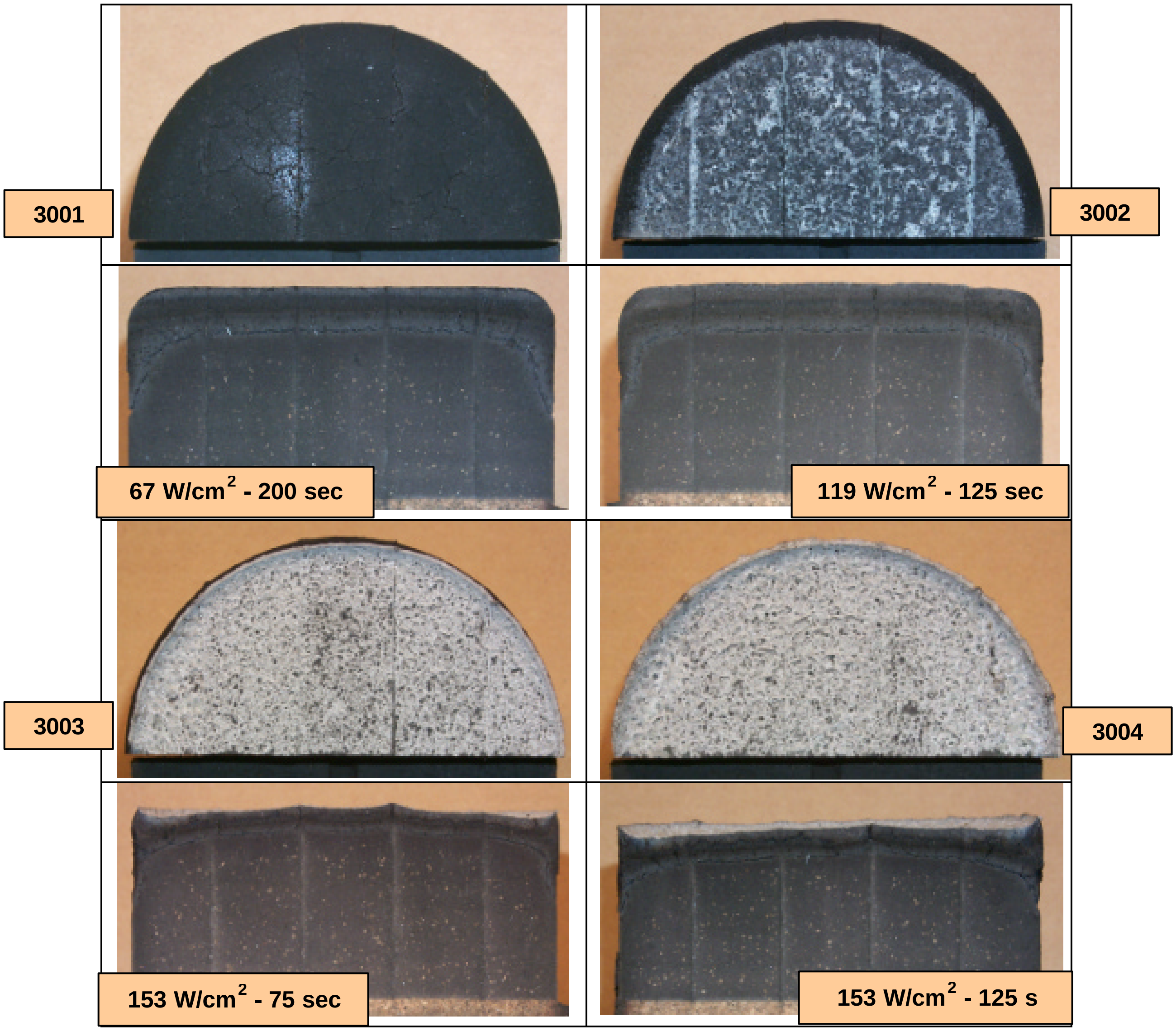

Fig. 5 – SRAM-20 (SCBA) Flat-Faced Samples Tested in the NASA/ARC IHF to 153 W/cm^2

Figure 6 shows four more 4.0-in. diameter SRAM-20 arc-jet samples tested in 2004 in the IHF (for thermal model correlation) at higher heating rates that involved higher levels of surface ablation and recession. (These samples, like those of Fig.4, were made with a rounded "iso-q" shape – 4.0-in. surface radius – whereas the samples of Fig. 5 had only a rounded shoulder of 0.25-in. radius and were otherwise flat faced.) Heating rates were 245, 311, 362 and 411 W/cm^2. Measured surface recessions in the same order were 0.185 in., 0.203 in., 0.233 in., and 0.221 in. (All sample surface recessions are summarized in Table 2.) SRAM-20 surface char layers become progressively thinner at increased heating rates. This is because surface ablation that consumes char is nearly matching the rate of char production from in-depth pyrolysis. Due to char-layer thinning, SRAM-20 becomes less efficient at high heating compared to other ablators such as the PhenCarb phenolic materials with denser chars. For example, PhenCarb-28 will maintain a thick char (shown below) at 411 W/cm^2, whereas SRAM-20 will not. Nevertheless, SRAM-20 performed well at all the high-heating conditions addressed by Figure 6 and the material showed no evidence of spallation or other performance shortfalls or "cliffs."

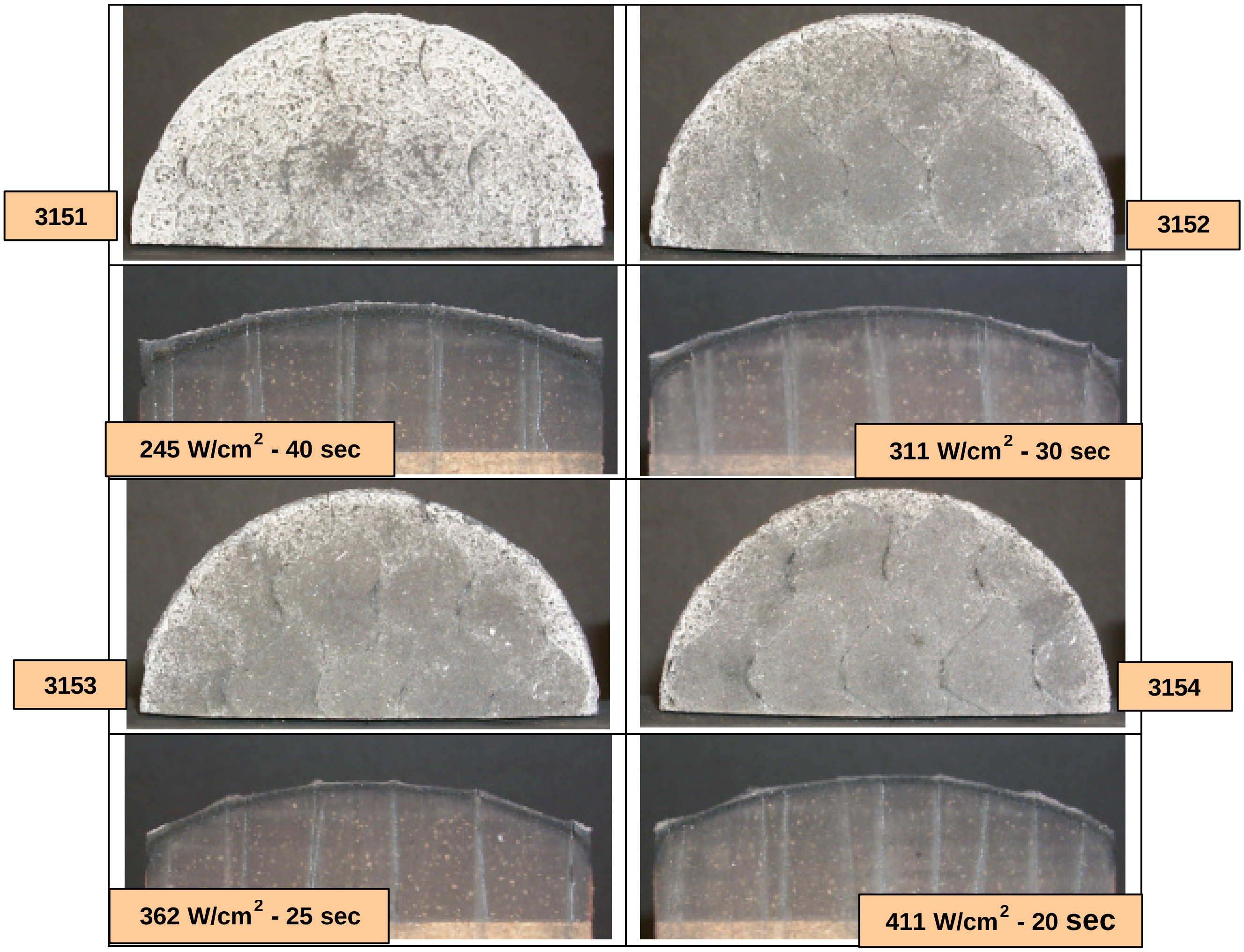

Fig. 6 – SRAM-20 (HCPA) Iso-Q Samples Tested in the IHF from 245 to 411 W/cm^2

Table 2 – Surface Recession for SRAM-20 Samples Tested from 119 to 411 W/cm^2

Sample	Heating / Time	Recession	Rec. Rate
3002	119 W/cm^2 / 125 sec	0.010 in.	0.00008 in./sec
3003	153 W/cm^2 / 75 sec	0.190 in.	0.00253 in./sec
3155	207 W/cm^2 / 60 sec	0.222 in.	0.00370 in./sec
3151	245 W/cm^2 / 40 sec	0.185 in.	0.00462 in./sec
3152	311 W/cm^2 / 30 sec	0.203 in.	0.00677 in./sec
3153	362 W/cm^2 / 25 sec	0.233 in.	0.00932 in./sec
3154	411 W/cm^2 / 20 sec	0.221 in.	0.01105 in./sec

D. PhenCarb-28 Detailed Discussion

The significantly more robust PhenCarb-28 ablator contains phenolic resin, reinforcing fibers, and low-density fillers, and is typically packed in large-cell honeycomb similar to SRAM-20. (And PhenCarb-28 is sometimes made from carbon H/C as well as silica H/C depending on heating.) Its final cured density in H/C is 28 lb/ft^3. P-28 has lower recession than SRAMs, but it is also heavier, more conductive, and has more complicated manufacturing.

Figure 7 shows posttest photographs of four sectioned PhenCarb-28 samples tested in the Ames IHF arc-jet at heating rates from 310 to 411 W/cm^2. These were 4.0-in. diameter samples with an initial thickness of 1.5 in. Their original shape was "iso-q" with a 4.0-in. convex surface. (For all "iso-q" samples, a curved surface yields uniform, constant heating, thus the meaning of the name, which is "constant q.") The P-28 ablator Sample 3170 heated for 40 sec at 411 W/cm^2 produced a thick, durable char

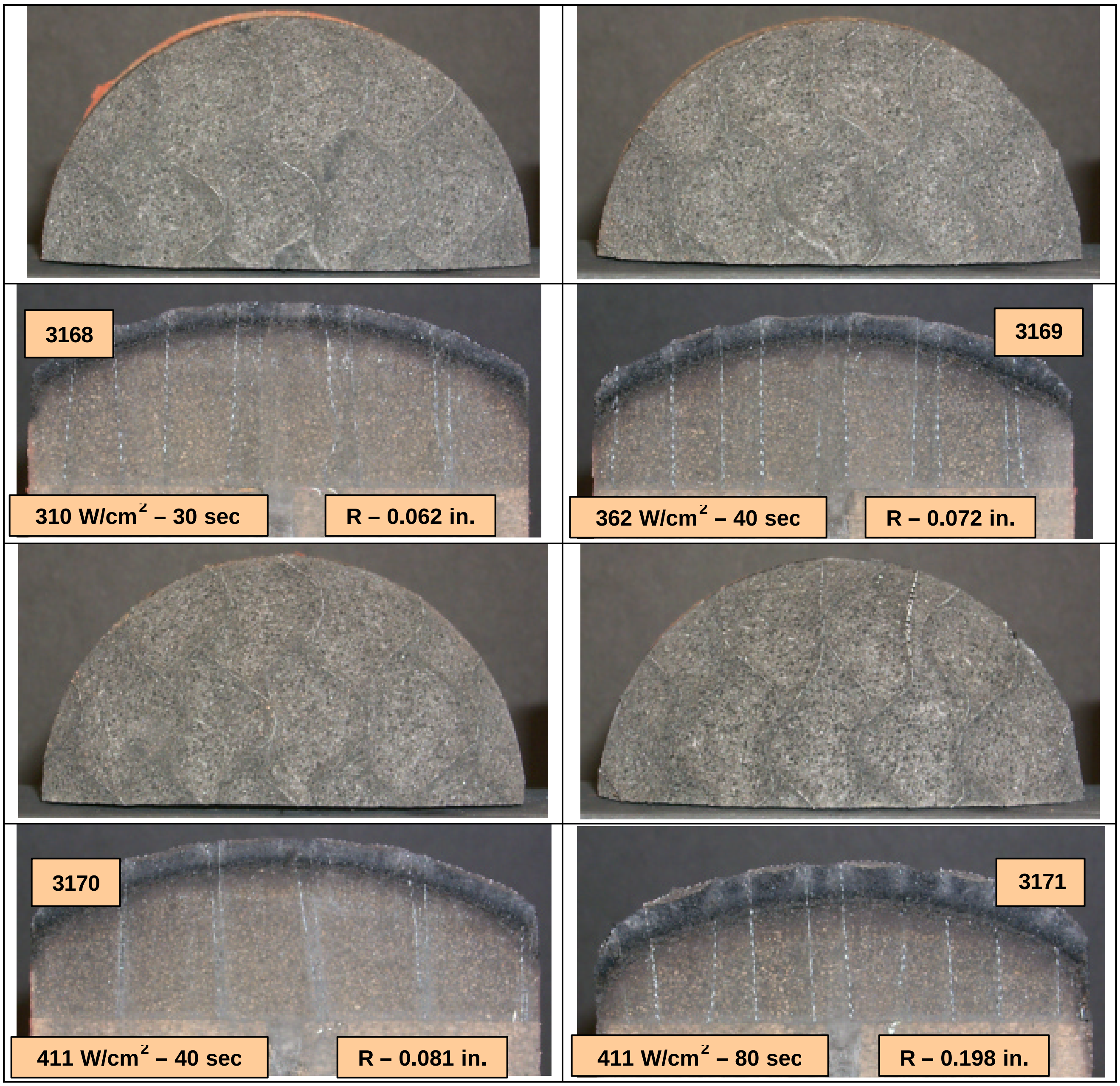

Fig. 7 – 4.0-In. PhenCarb-28 Samples (HCPA) Tested in the IHF Arc-Jet

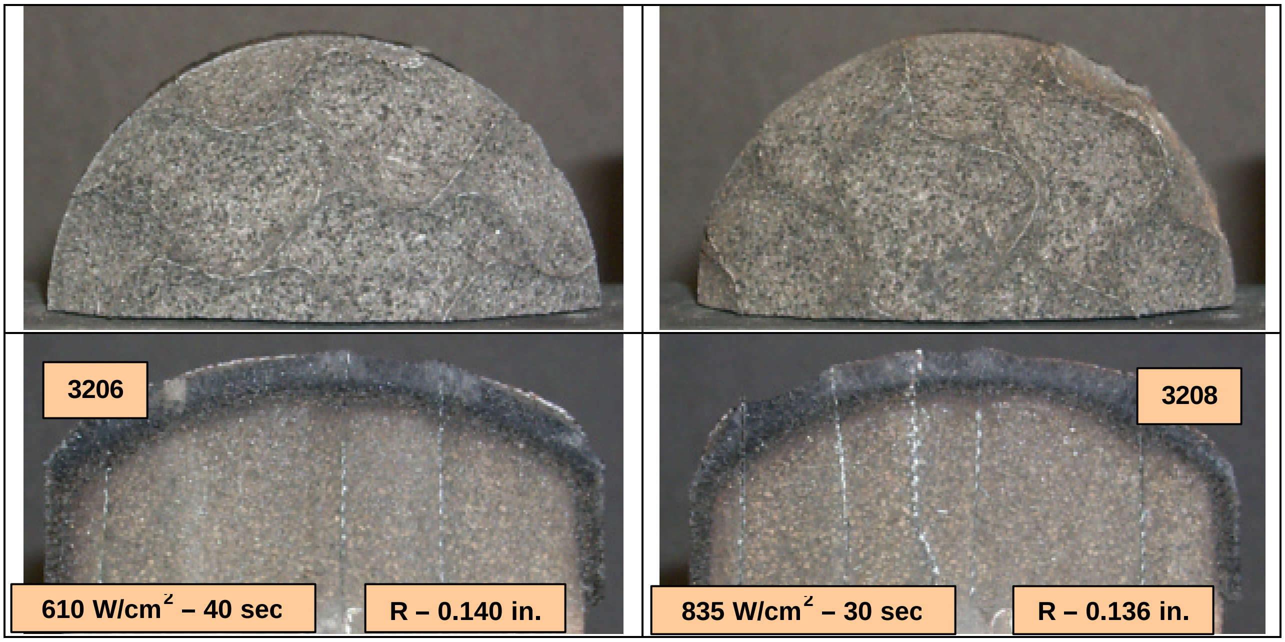

Fig. 8 – 3.0-In. PhenCarb-28 Samples (HCPA) Tested in the IHF Arc-Jet

layer while receding by only 0.081 in. The honeycomb material was carbon impregnated with phenolic resin. (Compare the thick char layer of this sample to that of SRAM-20 Sample 3154 tested at the same heating, which had a much thinner char – see Fig.6.) PhenCarb-28 Sample 3171 with identical make-up was tested for 80 sec at the same test condition. Again the sample produced a thick char layer and experienced a relatively low amount of surface recession of only 0.198 in.

Figure 8 shows posttest cross-section photos of additional PhenCarb-28 samples tested in the IHF at 610 W/cm^2 for 40 sec and 835 W/cm^2 for 30 sec. These samples had the same construction but were made smaller with a 3.0-in. diameter and 3.0-in. surface curvature. Sample 3206 tested at 610 W/cm^2 had a surface recession of approximately 0.140 in. Sample 3208 tested at 835 W/cm^2 had a recession of 0.136 in. Again, the ablator of these samples produced thick, durable char layers and provided excellent thermal protection to their substrates.

The primary function of honeycomb in charring ablators is to reinforce the char layer and prevent separation and loss of char during flight. However, PhenCarb-28, like Avcoat-5026 (the Apollo ablator), undergoes "coking," which further strengthens this already strong, reliable char layer. (Coking is carbon deposition in the char layer from percolating pyrolysis gases.) So much so, in fact, that we have successfully tested *monolithic* P-28 without honeycomb in the Ames arc-jets and observed very good performance. In these tests without honeycomb, there was no separation or mechanical loss of char in the P-28 samples (low shear, stagnation-type test environment). The possible flight application of P-28 without H/C is not advocated, but the monolithic tests certainly demonstrated its char stability and reliability. Figure 9 gives posttest photos of monolithic PhenCarb-28 samples that were tested at heating rates of 610, 835 and 1,003 W/cm^2. Sample 3220 tested at 835 W/cm^2 for 40 sec produced a surface recession of 0.232 in. Sample 3222 tested at 1003 W/cm^2 for 30 sec had recession of 0.169 in. The char layers on all of these monolithic samples shown in Figure 9 were thick, uniform, and relatively smooth, all characteristics that are highly desirable. ARA's extensive arc-jet test program over the past four years, demonstrated that PhenCarb-28 (and its family homologues) could reliably perform entry missions at heating up to 1000 W/cm^2. In addition, the P-28 ablator is tough and relatively forgiving in terms of surface nicks and dings. And small, inadvertent dings – while they might locally increase heating due to interference effects – will not significantly degrade ablator performance as might occur, for example, in a C-SiC system when its outer layer is breached.

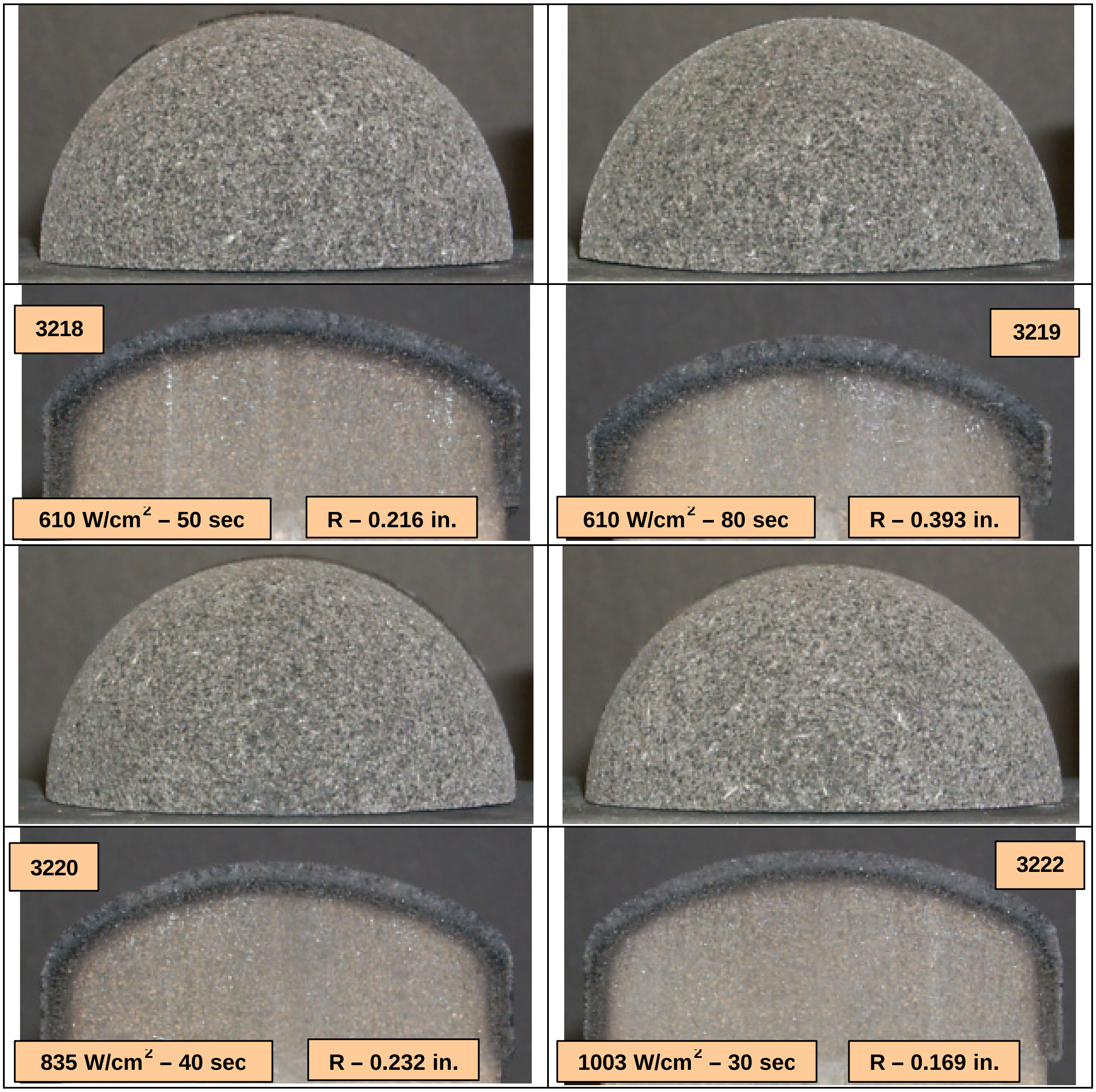

Fig. 9 – 3.0-In. PhenCarb-28 Samples (Monolithic) Tested in the IHF Arc-Jet

E. Ablator Production

As shown above, SRAM-20 and PhenCarb-28 are most commonly produced by honeycomb packing using custom large-cell honeycomb. (This H/C provides a better end product for these ablators than the commercially-available, small-cell system now in use for Mars vehicles.) Figure 10 shows this standard large-cell honeycomb produced in the Ablatives Lab solely for ablator manufacturing. The H/C uses flexible cell geometry, sometime known as "flex core", that allows the H/C sheets to bend in two directions and conform to sphere-cone aeroshell shapes. (Apollo honeycomb was hexagonal cell and less flexible.) The cell size, or cross-dimension, is approximately 1.0-in. and the area of each cell is roughly equivalent to a standard postage stamp (shown). The H/C sheet in the photo is "lab size" for making arc-jet samples. Its dimensions are 15.5 in. by 14.0 in. The H/C material shown is a silica phenolic, but carbon-phenolic honeycomb is produced with the same equipment and has approximately the same appearance.

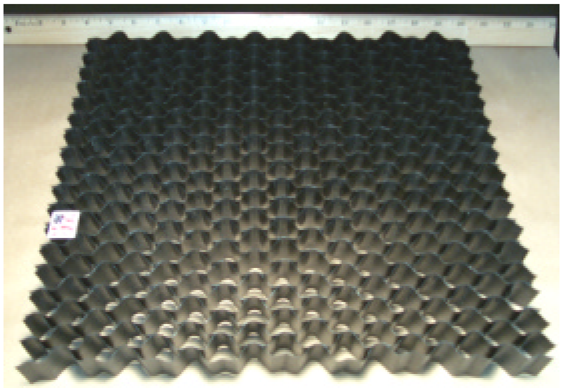

Fig. 10 – ARA Large-Cell Honeycomb (HCPA)

The SRAM-20 and PhenCarb-28 ablators in honeycomb are produced by two methods. One method ("conventional") is to first bond the H/C sheet to structure (i.e., aeroshell surface), followed by packing the H/C cells with ablator compound, then applying an overpack layer, followed by curing. A second method is to pack and cure "free-standing" honeycomb on a pre-form or caul plate. After cure, the ablator is then lifted from the form and secondarily bonded to structure. (Because a *modular* heatshield would need to use this second method, the method is commonly referred to as "modular.") In both methods curing is accomplished by vacuum bag pressure and elevated temperature. One advantage of the second method is that honeycomb sheet can be pressed down through an initial layer of ablator compound that has already been evenly applied to the preform, thus facilitating packing and production. For thick honeycomb, this can help assure full-density ablator at the bottom of the H/C cells. An alternate to the second method is to pack and cure free-standing honeycomb in a mold using the mold's upper platen to apply compaction and cure pressure instead of a vacuum bag. A cured panel segment of P-28 in silica H/C is shown in Figure11.

As stated above, the primary purpose of honeycomb is to stabilize the char layer during entry and prevent mechanical separation and loss of char from the surface. Char loss would produce a rough surface and cause interference heating in addition to loss of insulation. However, honeycomb can serve another function besides char stabilization. In some applications (e.g., SLA-561v production) it is used to control ablator thickness during manufacture. Here the H/C sheet is made to design thickness with required tolerance and then the packed and cured ablator (with overpack) is sanded or milled down to the top of the H/C sheet. However, both SRAM-20 and PhenCarb-28 use honeycomb for enhancement of char stability only. This is because ablator production at the Ablatives Laboratory relies on CNC milling to control ablator thickness both for test samples and for full aeroshells.

Fig. 11 – Cured PhenCarb-28 (HCPA) Panel

F. Aeroshell Manufacturing

The Ablatives Laboratory will use conventional honeycomb packing as the primary approach for manufacturing the SRAM and PhenCarb heatshields for spacecraft missions. A completed 1.0-meter diameter SRAM-20 aerocapture aeroshell and its manufacturing steps are shown in Figure 12. This process uses the standard custom-made, honeycomb shown above with a 1.0-in. cell size (silica-fabric with phenolic resin). The formed honeycomb is fitted and then bonded to the aeroshell structure with film adhesive. Curing is accomplished under vacuum bag at oven temperature. Next the ablator compound is mixed and packed into the honeycomb cells followed by another cure cycle under vacuum bag at oven conditions. The final step is precision CNC milling to final aeroshell shape and ablator thickness. (Note in the "packing" photo of Figure 12 that the aeroshell has a base extension that is later machined away. This extension technique produces a stable, reliable cone edge on the final aeroshell.)

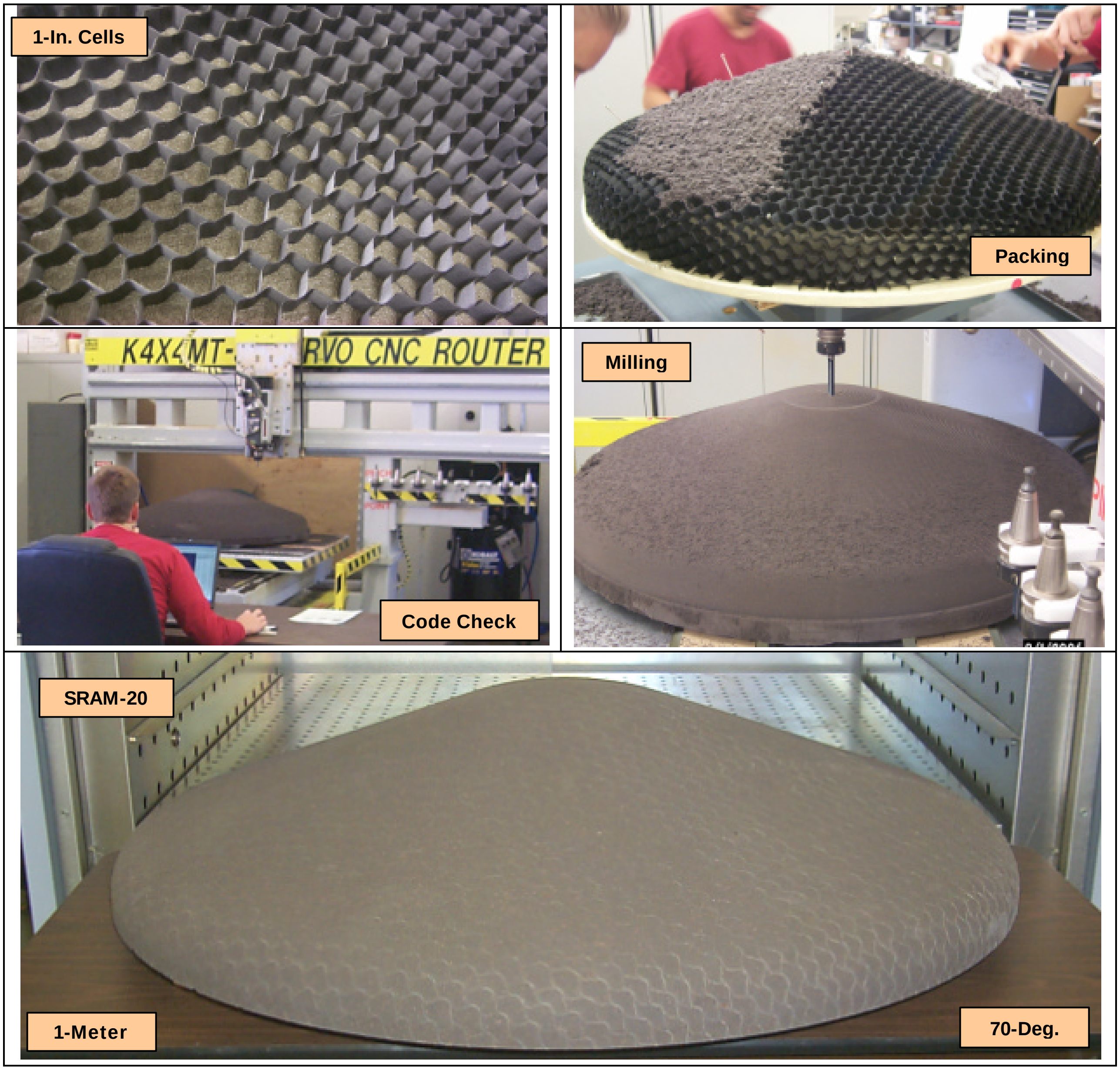

Fig. 12 – Manufacturing of 1.0-Meter SRAM-20 (HCPA) Aeroshell

G. System Thermostructural Testing

The SRAM-20 aeroshell system will experience surface temperatures up to about 1930ºC (3500ºF) along with steep temperature gradients through the ablator thickness down to its structure, which will have a temperature approaching the maximum bondline allowable of 250ºC (481ºF). Thus, the ablator is expanding at its high temperature while the composite structure beneath is relatively cool. This creates high thermal stresses in the bondline that could potentially cause debonding and separation of the ablator from its aeroshell structure. It is important to test aeroshell heatshield systems to verify that debonding and failure will not occur. For the aerocapture aeroshell design of this paper such testing has been done (and is still on-going) at the Sandia Solar Tower facility at Kirtland AFB.

The Solar Tower (ST) has a field of 220 heliostats with reflective mirrors that track the sun and focus its collected energy at the tower down to a spot size as small as approximately

1.0-m (39.4 in.). The total area of mirrored surfaces is 2.2 acres or 88,000 ft^2. Heatshield test articles placed within this concentration spot can be subjected to thermal radiation flux levels as high as 300 W/cm^2 (for ideal conditions).

Under ISPT efforts, ARA has been testing ablator samples at ST since 2003, first to characterize their responses to intense thermal radiation (for radiation-dominated entry environments [9-12]) and more recently for verification of ablator-system thermostruc-tural integrity. ST is really the only facility available today in the U.S. that can test large-size ablator test articles at high flux levels. Today's arc-jets cannot do this testing due to power limitations. The open-air ST has the added advantage that it vents all ablation products to the atmosphere and thus prevents contamination of facility hardware that would occur in an arc-jet or other in-door facility.

To date we have tested six 24-in. by 24-in. panels of SRAM-20 over composite structure (flight-like design for Earth aerocapture) and three similar PhenCarb-28 panels at the ST to evaluate system thermostructural integrity for a 250ºC (481ºF) bondline allowable temperature. Figure 13 provides a visual summary for one of the SRAM-20 tests conducted in October of 2006. All of these ablator panel tests were limited to a standardized solar heat flux of about 150 W/cm^2 due to concerns for some potential malfunctioning of heliostats and some possible weather-related power losses. The SRAM-20 panel with composite structure of Figure 13 was tested at a square pulse of 154 W/cm^2 for a duration of 210 sec. (The objective in these panel thermostructural tests was not to closely match the predicted flight heating environment but, instead, to apply the large available heat source to raise the panel's bondline temperatures to flight-allowable levels within flight-similar timelines.)

In the left side of the Figure 13 is a photo of SRAM-20 Panel 471 taken during the radiation exposure. The 24-in. by 24-in. test panel is mounted at the top of a water-cooled fixture that sits atop the facility's 200-ft tall tower. Within this photo, the concentrated radiation is coming from the right from ground-level heliostats that

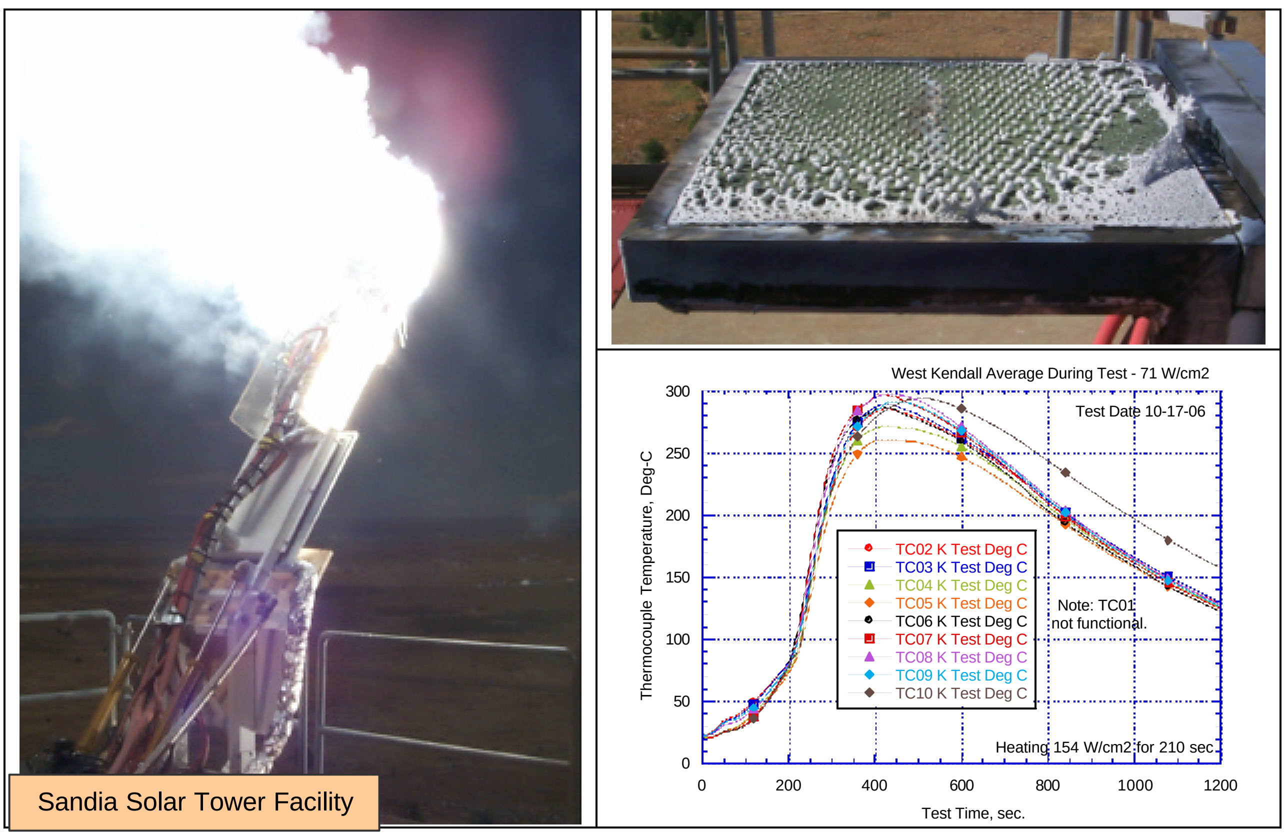

Fig. 13 – Photos of HCPA SRAM-20 Panel 471 (24-in. by 24-in.) in Test at 154 W/cm^2 for 210 sec with Posttest Surface Appearance and Plotted Bondline Temperatures

are looking up at the test article. A large cloud of ablation products from the test surface is flowing to behind the panel's test fixture. In the upper right-hand side of the figure is the posttest appearance of the surface of Panel 471. SRAM-20 is a high-silica material and the posttest surface shows regions of "condensed" silica that had percolated to the surface during the intense exposure. This panel contained ten bondline thermocouples spread out across its total area. There are commonly some variations in T/C responses due to ambient wind effects and local scattering of solar radiation by the cloud of formed ablation products. However, all of the working T/C's of this test panel recorded bondline peak temperatures of 250ºC or greater, the defined maximum allowable for this system test. The test was successful in that no debonding occurred and the system remained intact for temperatures at or above the bondline allowable. This was confirmed by on-site inspection of the panel following test and by follow-on sectioning of the panel in the laboratory. The other similarly tested panels showed the same successful performance of the SRAM-20 system.

III. SUMMARY DISCUSSION

The Ablatives Laboratory has been maturing new family systems of ablators for the past four years under ISPT sponsorship. These materials have diversity of density and performance to cover a broad range of predicted entry-heating environments for upcoming spacecraft. The goal has been to raise their technical readiness levels to TRL-6 to make them ready for infusion as the TPS for NASA deep-space missions (planets and Titan). Since 2003, over 300 arc-jet tests have been conducted in the NASA/ARC facilities for ablator-families performance characterization and thermal modeling. In addition, their thermal radiation responses – such as radiation penetration, ablation, and resistance to spallation – have been tested through more than 100 cylindrical-sample tests at the Solar Tower facility. (These tests used a subsonic wind tunnel to sweep away ablation products and a large quartz window for entry to the tunnel of high-flux radiation at 150 W/cm^2.) Large panels and sub-scale, shaped aeroshells are also being tested atop Solar Tower for the purpose of thermostructural validation of the ablator-structure systems to defined bondline temperature allowables (e.g., 250ºC). Today a number of the new ablators have achieved a sufficiently high TRL that they are candidates for flight infusion. The SRAM-20 silicone ablator for example was competitively selected and baselined by NASA in 2006 for flight validation on a future Earth-aerocapture flight test. Also, 1.0-m demonstration (and test) aeroshells have been produced to date and, under ISPT, a larger 2.65-m aeroshell (MPF/MER size) will be manufactured and tested in the coming year against launch and flight environments.

IV. ACKNOWLEDGMENT

The work described in this paper was funded in whole or in part by the In-Space Propulsion Technologies Program, which is managed by NASA's Science Mission Directorate in Washington, D.C., and implemented by the In-Space Propulsion Technology Projects Office at Glenn Research Center in Cleveland, Ohio. The program objective is to develop in-space propulsion technologies that can enable or benefit near and mid-term NASA space science missions by significantly reducing cost, mass and travel times.

V. REFERENCES

1. W.M.Congdon and D.M.Curry, "Thermal Performance of Advanced Charring Ablator Systems for Future Robotic and Manned Missions to Mars," AIAA Paper No. 2001-2829, 35th AIAA Thermophysics Conference, Anaheim, CA, June 2001.
2. W.M.Congdon and D.M.Curry, "Arc-Jet Testing and Thermal-Response Modeling of Advanced Lightweight Charring Ablators," Paper No. 2002-2999, 8th AIAA/ASME Joint Thermophysics and Heat Transfer Conference, St.Louis, MO, June 2002.
3. W.M.Congdon, D.M.Curry, and T.J.Collins, "Response Modeling of Lightweight Charring Ablators and Thermal Radiation Testing Results," AIAA Paper No, 2003-4657, AIAA Joint Propulsion Conference, Huntsville, AL, July 2003.
4. B.Laub, D.Curry, "Tutorial on Ablative TPS," NASA Ames Research Center Workshop, 2nd International Planetary Probe Workshop, NASA Ames Research Center, Moffett Field, CA, August 2004.

5. B.Laub, “TPS Materials & Systems for Human and Robotic Exploration Missions,” Technical Presentation at Human & Robotic EDL Capabilities Workshop, NASA Ames Research Center, Moffett Field, CA, February 2005.
6. B.James, M.Munk, and S.Moon, “Development of Aerocapture Technologies,” AIAA Paper No 2002-2103, 17th AIAA Aerodynamic Decelerator Systems Technology Conference, Monterey, CA, May 2003.
7. J.L.Hall, “Aerocapture (Vol.I) Concept Definition Study Report,” NASA/JPL Contract Report for New Millennium Program Space Technology (ST9), NRA NNH04ZSS002N, August 2006.
8. B.Laub, “Thermal Protection Concepts and Issues for Aerocapture at Titan,” AIAA Paper No. 2003-4954, AIAA Joint Propulsion Conference, Huntsville, AL, July 2003.
9. J.Olenjniczak, D.Prabhu, M.Wright, N.Takashima, D.Hollis, and K.Sutton, “An Analysis of the Radiative Heating Environment for Aerocapture at Titan,” AIAA Paper No. 2003-4953, AIAA Joint Propulsion Conference, Huntsville, AL, July 2003.
10. M.J.Wright, D.Bose, and J.Olejniczak, "The Impact of Flowfield-Radiation Coupling on Aeroheating for Titan Aerocapture," *Journal of Thermophysics and Heat Transfer*, Vol. 19, No. 1, 2005, pp. 17-27.
11. D.Bose, M.J.Wright, G.Raiche, D.Bogdanoff, and G.A.Allen, "Modeling and Experimental Validation of CN Radiation Behind a Strong Shock Wave," AIAA Paper No. 2005-0768, Jan. 2005. Accepted for publication in the *Journal of Thermophysics and Heat Transfer,* July 2005.
12. M.J.Wright, “Latest Titan Heating Rates (Peaks),” NASA/ARC Technical Memorandum, Nov. 2005.

William M. Congdon
18 May 2007